Materials and Design 31 (2010) 808–815

Contents lists available at ScienceDirect

Materials and Design

journal homepage: www.elsevier.com/locate/matdes

Mechanical and swelling properties of thermoplastic elastomer blends

M. Abu-Abdeen *, I. Elamer

Physics Department, Faculty of Science, King Faisal University, P.O. Box 400, Al-Hassa 31982, Saudi Arabia

ARTICLE INFO

Article history:
Received 30 April 2009
Accepted 29 July 2009
Available online 14 August 2009

Keywords:
Elastomers
Thermoplastics
Blends
Stress–strain
Microhardness
Swelling

ABSTRACT

The mechanical behavior, microhardness and abrasion resistance of acrylonitrile butadiene rubber (NBR) vulcanizate loaded with 40 phr fast extrusion furnace (FEF) carbon black nanopowder and different concentrations of suspension polymerization polyvinyl chloride (PVC) were studied. The measured parameters (i.e., the Young's modulus, tensile strength, and elongation at break) varied with the concentration of PVC. Both the elastic modulus and the tensile strength increased with increasing PVC loadings while the elongation at brake recorded a linear decrease. The hardness degree and the abraded mass increased as the concentration of PVC increased. The classical theory of rubber elasticity was used to calculate the rubbery modulus, the number of effective chains per unit volume and the average molecular weight. Swelling measurements were done on the mentioned samples. Addition of PVC was found to decrease the maximum degree of swelling, the penetration rate and the average diffusion coefficient. Swelling was found to slightly affect the degree of hardness and elastic modulus.

1. Introduction

Considerable research interest is focused on new polymeric materials obtained by blending two or more polymers [1]. The major feature of such a process is that the intermediate properties are in some cases better than those exhibited by either of the single components. In addition, some modification in terms of processing characteristics, durability, and cost can be achieved via polymer blending. The modification in the behavior of polymer systems has been the subject of many studies [2,3]. Poly(vinyl chloride)/nitrile butadiene (PVC/NBR) blends are perhaps the oldest commercial blends, having been introduced about 60 years ago [4]. It is worth noting that NBR acts as a permanent plasticizer for PVC in applications such as wire and cable insulation in which PVC improves the chemical resistance, thermal ageing and abrasion resistance of NBR. Furthermore, PVC forms a miscible blend with NBR as evidenced from a single glass transition temperature (T_g) which is intermediate between that of the pure components and so PVC/NBR can be considered as a melt processible thermoplastic rubber [5,6].

The many attractive mechanical characteristics of polymer blends have made it desirable to choose these materials over traditional materials for numerous types of applications, such as binder constituents in explosives, load-bearing components, and jet engine modules. As the uses of polymer blends increase, an understanding of the mechanical behavior of these materials becomes vital for creating innovative and economical designs for various components. Polymer blends have more complicated properties as they display elastic and viscous responses at different strain rates and temperatures [7,8].

Polymer blends are usually nonresistant to oils, greases, or fuels and therefore are swollen by them. This causes changes in their mechanical characteristics (particularly their moduli and loss angles) and shortens the time of exploitation [9,10]. There are lot of papers concerning the influence of many factors on the mechanical and the dynamic properties of rubber blends [9–11]. However, only few of them take into account the significance of the problem (practically and theoretically) of the influence of swelled vulcanizates by liquids on their mechanical properties.

The interaction of polymeric materials with different solvents is an important problem from both the academic and technological points of view [12–14]. Crosslinked polymers brought in contact with different solvents during service applications usually exhibit the phenomenon known as swelling. The capacity of crosslinked polymers for the degree or the amount of swelling assesses swelling expressed as the amount of liquid absorbed by the polymer. The swelling properties of polymers are mainly related to the elasticity of the network, the extent of crosslinking, and the porosity of the polymer [15,16]. The determination of the resistance of a polymer to solvents and gases is standardized in test procedures before the polymer finds successful applications involving exposure to such solvents and gases [17,18].

On the other hand, the hardness degree measurement may be important for assessing product performance and is used in

* Corresponding author. Address: Physics Department, Faculty of Science, Cairo University, Giza, Egypt. Tel.: +966 534066436.
E-mail address: mmaabdeen@yahoo.com (M. Abu-Abdeen).

0261-3069/$ - see front matter © 2009 Elsevier Ltd. All rights reserved.
doi:10.1016/j.matdes.2009.07.059

identifications, classifications and quality control of products. Hardness tests provide a rapid evaluation of variations in mechanical properties affected by changes in chemical or processing conditions, addition of compounding ingredients, heat treatments, swelling, ageing and microstructure of the samples. Microhardness measurement offers a nondestructive technique for studying the mechanical behavior of materials and its application to polymeric materials is widely utilized now [19].

The objective of this work was to study the effect of adding polyvinyl chloride (PVC) to acrylonitrile butadiene rubber (NBR) loaded with the percolation concentration of fast extrusion furnace (FEF) carbon black on uniaxial stress–strain behavior under tension, hardness degree, abrasion resistance and swelling properties. We also sought to develop a simple and flexible phenomenological constitutive model to characterize the observed dependence of the mechanical behavior and swelling properties on the concentration of PVC.

2. Experimental

2.1. Materials

Commercial grades of both acrylonitrile butadiene rubber NBR (acrylonitrile content of 33%, with specific gravity of 0.990 ± 0.005 and Moony viscosity (ML4) of about 45 at 373 K) were purchased from Alexandria Trade Rubber Company (TRENCO, Alexandria, Egypt). Polyvinyl chloride (PVC) was purchased from Sabic, Saudi Arabia. Fast Extrusion Furnace (FEF) carbon black-N550, ASTM designation, particle size diameter ranges from 40 to 48 nm, ASTM D1765-86, and average specific area 40–49 m^2/g (ASTM D1765-96) was used as reinforcement filler. Other compounding ingredients like zinc oxide and stearic acid (activators), dibenzothiazyl disulphide (MBTS) semi-ultra accelerator, phenyl-naphthylamine (PBN) antioxidant (melting point 105 °C), dioctyle phthalate (DOP) plasticizer and sulfur (vulcanizing agent) were used. These materials were compounded according to the recipe listed in Table 1. The compounds were mixed according to ASTM D 3182 in a laboratory-sized mixing mill at a friction ratio of 1:1.19 by careful control of the temperature, nip gap, time of mixing, and uniform cutting operation for 30 min. After mixing, the rubber compositions were molded in an electrically heated hydraulic press to the optimum cure with molding conditions that were previously determined from torque data with a Monsanto R100 rheometer (New York). Details of compounding and vulcanization process can be found elsewhere in a previous work [19].

Table 1
Mix formation of 40FEF/NBR vulcanizates loaded with PVC.

Ingredients (phr)[a]	Concentration (phr)									
	M0	M1	M2	M3	M4	M5	M6	M7	M8	M9
NBR	100	100	100	100	100	100	100	100	100	100
FEF	40	40	40	40	40	40	40	40	40	40
Processing oil	10	10	10	10	10	10	10	10	10	10
Stearic acid	2	2	2	2	2	2	2	2	2	2
MBTS[b]	2	2	2	2	2	2	2	2	2	2
PBN[c]	1	1	1	1	1	1	1	1	1	1
Zinc oxide	5	5	5	5	5	5	5	5	5	5
Sulfur	2	2	2	2	2	2	2	2	2	2
PVC	0	10	20	30	40	50	60	70	80	90

[a] Parts per hundred parts of rubber by weight.
[b] Dibenzothiazyle disulphide.
[c] Phenyl-*b*-naphthylamine.

2.2. Testing

2.2.1. Tensile tests

The tensile tests were determined on a dumbbell-shaped specimens. The measurements were carried out at 25 °C on an Instron 3345J8621 (Norwood) tensile machine with a grip separation of 40 mm at a crosshead speed of 500 mm/min per ASTM D 412 and ASTM D 624, respectively.

2.2.2. Microhardness test

The hardness (Shore A) of the studied samples was determined with a Zwick/Roell 3130/3131 DGM 93 18 389.5 hardness tester (Ulm, Germany) in accordance with ASTM D 2240-05. The tests were performed on samples 30 mm in diameter and 6 mm thick. The readings were taken after 10 s of indentation after firm contact had been established with the specimen.

2.2.3. Abrasion test

Abrasion loss of the samples was measured using a Y571L Rubbing Instrument (Laizhou Electron Instrument Co., Ltd., Laizhou, China), taking 400 times of friction as a test circle, so the total abraded mass rubbed away from the surface of the samples was obtained in the circle. Three samples were tested for each data point and the average abraded mass was calculated.

2.2.4. Swelling test

Blends were weighed and inserted into test tubes containing a solvent at constant temperature. The blends were removed from the solvent and blotted with filter paper to remove excess solvent from the surface of the sample. The blends were then weighed to an accuracy of 0.1 mg at a given time and at a fixed temperature. The equilibrium-swelling ratio, Q, was calculated by using the gravimetric method, where Q is given by

$$Q = \frac{M_t - M_r}{M_r} * 100\% \quad (1)$$

where M_t is the mass of the sample after swelling at time t and M_r is the mass of dry sample before swelling.

3. Results and discussion

3.1. Stress–strain curves

The stress–strain curves of 40FEF/NBR vulcanizates loaded with different concentrations of PVC are illustrated in Fig. 1. These curves are typical of elastomeric materials, with no well-defined yielding point and a long plastic flow region. At low strains the kinetic theory holds. At large deformations, there is limited extensibility of the crosslinked chains. Meanwhile, there is a stress-softening effect at moderate strains. Separate plots of the change in stress and strain (not shown here) $d\sigma/d\varepsilon$ versus strain ε were determined for all PVC loadings. They showed strain-independent regions at very low strain values. These constant values are taken to be Young's modulus (E) at different PVC loadings, which are shown in Fig. 2. Loadings of PVC up to approximately, 30 phr do not affect the values of E. In this region no any reactions are present between NBR and PVC. Slight increase in E is observed at concentrations between 40 and 60 phr which may indicates the formation of weak Vander Waal bonds. A sharp increase is observed at concentrations of PVC greater than 60 phr. Such a trend indicates that incorporation of PVC into 40FEF/NBR vulcanizates increases the stiffness of the blend.

The effect of PVC loadings on the tensile strength (σ_b) for PVC–NBR blend vulcanizates loaded with 40 phr FEF is shown in Fig. 3. A sharp decrease in σ_b from 12.56 MPa at zero concentration of PVC

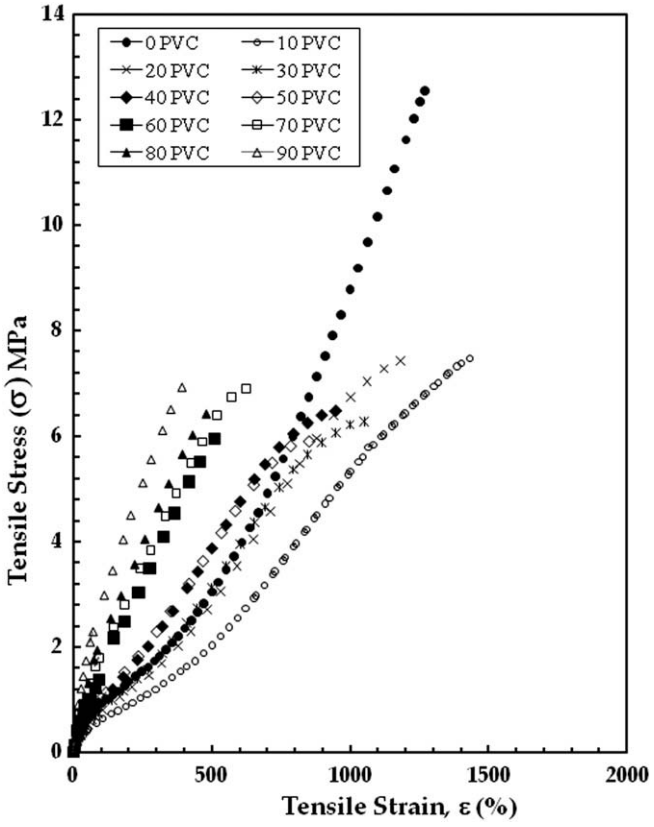

Fig. 1. Stress–strain curves for 40FEF/NBR loaded with different concentrations of PVC.

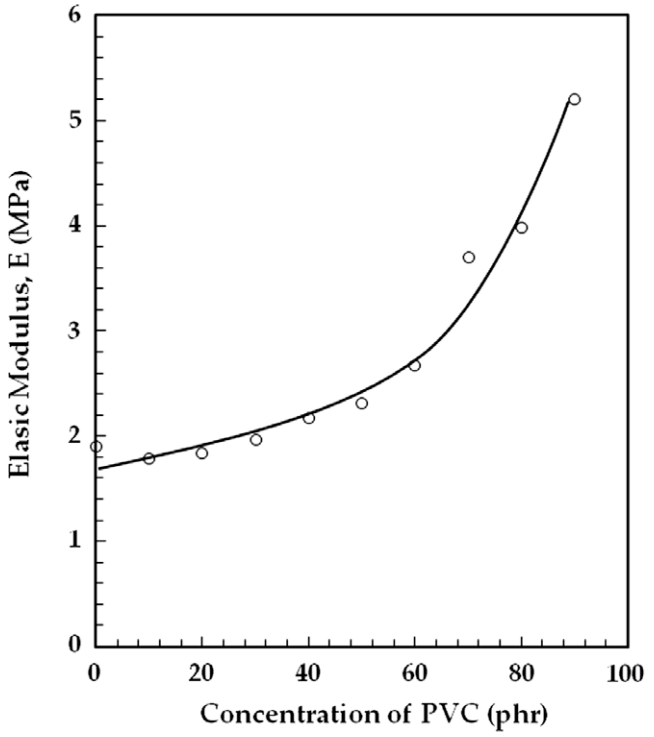

Fig. 2. The elastic modulus for 40FEF/NBR loaded with different concentrations of PVC.

to 7.47 MPa at a loading of 10 phr followed by a slight decrease at loadings of PVC between 10 and 50 phr are observed. This trend

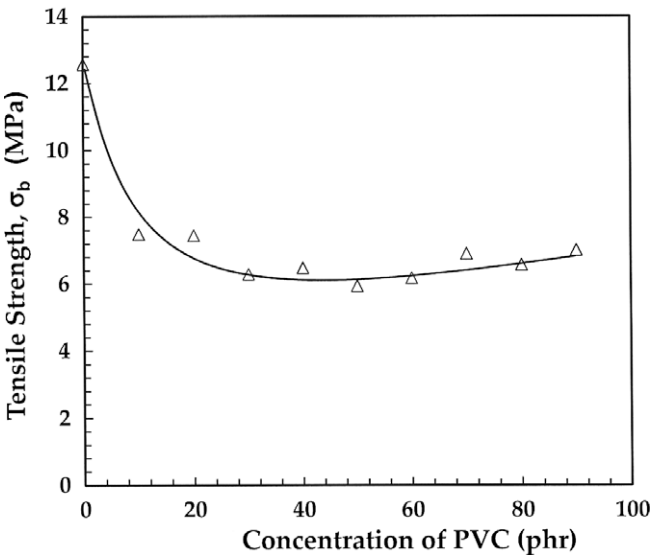

Fig. 3. The tensile strength for 40FEF/NBR loaded with different concentrations of PVC.

could be associated with the poor wetting of the PVC by the rubber matrix. This poor wetting will lead to poor interfacial adhesion between the PVC and rubber matrix resulting in weak interfacial regions. At concentrations beyond 50 phr of PVC σ_b slightly increase again as a formation of some bonds between PVC and NBR which is named co-vulcanization. This is also, mainly due to improved adhesion between the PVC–rubber matrices. This would result in reduced interfacial regions and stronger interfacial bond. It would therefore be anticipated that more efficient stress transfer would occur between the PVC as a load is applied [20].

Fig. 4 shows the dependence of elongation at break (σ_b) on the concentration of PVC in 40FEF/NBR vulcanizates. The addition of PVC found to reduce the elongation at break drastically. Such a decline is associated with the decreased deformability of a rigid interphase between the PVC and the matrix material.

3.2. Microhardness

Fig. 5 illustrates the dependence of the difference in the hardness degree with the concentration of PVC incorporated in 40HAF/NBR vulcanizates. It shows an increase approximately comparable with the change in E with PVC loadings. The degree of hardness (H) is related to E according to the following relation [19]:

$$\frac{E}{E_0} = \frac{mH}{100 - mH} \tag{2}$$

where E and E_0 are the tensile elastic moduli for the loaded PVC and unloaded samples, respectively, and m is a conversion factor, the value of which is determined with $E/E_0 = 1$ and $H = 61.275$ for an unloaded sample. The value of m was found to equal 0.81. Fig. 6 shows the variation of E/E_0 and H/H_0 (where H and H_0 are the hardness degrees of loaded and unloaded samples, respectively) with the concentration of PVC. A good agreement between the values from Eq. (2) and the experimental values of E displayed previously in Fig. 2 is observed. The behavior of E and H indicates that there is an enhanced polymer concentration at the interfacial region between PVC–NBR phases of the compatibilized blends. The increase in the PVC concentration at the interfacial region will facilitate the co-vulcanization between PVC and NBR. The co-vulcanization increases the interfacial adhesion between the PVC and NBR phases. An applied load can be transferred across the strengthened inter-

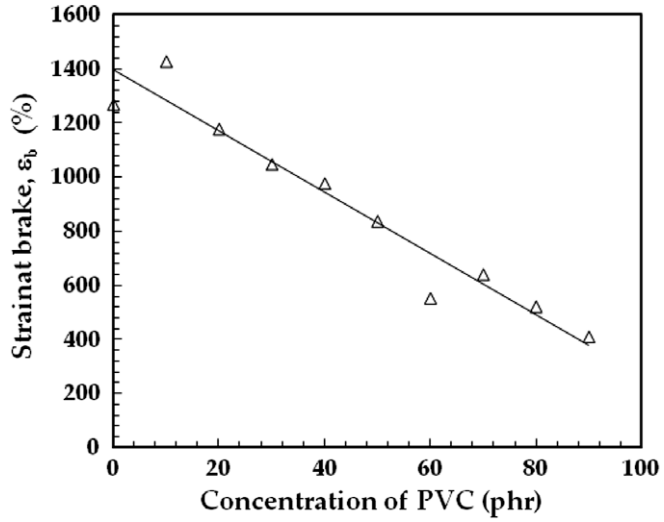

Fig. 4. The strain at brake for 40FEF/NBR loaded with different concentrations of PVC.

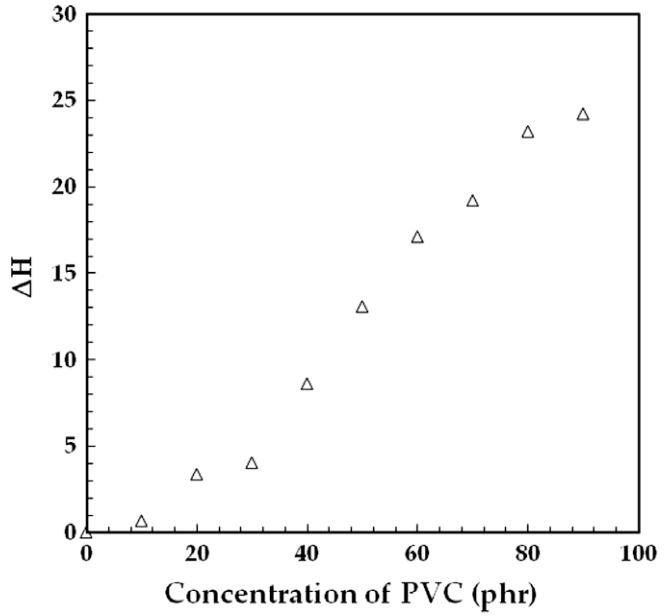

Fig. 5. The change in the degree of microhardness for 40FEF/NBR loaded with different concentrations of PVC.

face, resulting in higher elastic modulus and hardness. In the blends without any compatibilizer, the weak interface cannot withstand any high load, leading to small *E* and *H*.

3.3. Abrasion resistance

The friction and abrasion of polymer materials is a complex and dynamic process, closely related to hardness, toughness, fatigue, and so on. Fig. 7 shows the abrasion loss (as a loss of mass) as a function of PVC loadings. At low concentrations up to 30 phr of PVC the abrasion resistance has a small decrease. At concentrations between 30 and 40 phr, there is an abrupt decrease followed with another small decrease at concentrations less than 70 phr from PVC. At concentrations greater than 70 phr of PVC the abrasion resistance has a slight increase. The abrasion surface of the pure 40HAF/NBR has a lot of debris rubbed off. During the course of

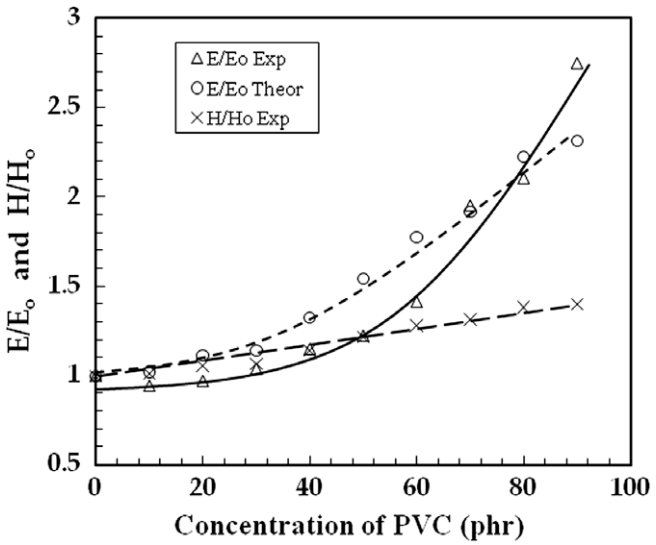

Fig. 6. Dependence of both E/E_0 and H/H_0 for 40FEF/(PVC–NBR) on the concentrations of PVC.

the abrasion experiment, some thin debris was extracted from the pure samples. This showed that the abrasion mechanism of the pure samples can be mainly attributed to severe adhesive abrasion, which occurs between the soft polymer surface and the hard and rough surface of the counterpart. According to adhesive abrasion theory, the friction between 40HAF/NBR sample and sandpaper on a grinding wheel produces a "planing" effect on the samples by the rough peaks of the sandpaper surface. It is very difficult to form a stable transfer film on the surface. Therefore, in the process of abrasion, adhesion easily happens [21]. At the same time, in the course of repeated friction, heat is generated. As a result, the temperature will be elevated, and the sample surface will undergo thermoplastic deformation under the friction stress [21]. Consequently, the abrasion loss of the pure samples is relatively large. These processes are much effective as PVC added. Furthermore, when the PVC content is increased, the NBR is unable to fill the gaps between the PVC particles, and so the continuity of the matrix is undermined. This leads to a decrease in the abrasion

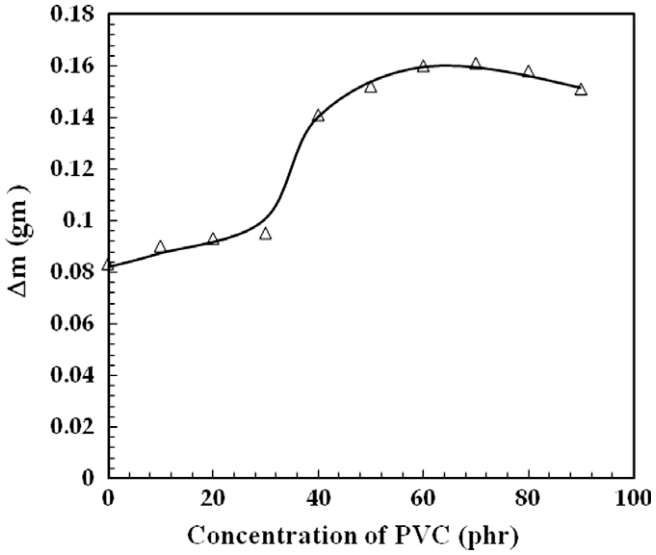

Fig. 7. Dependence of the abraded mass for 40FEF/(PVC–NBR) on the concentrations of PVC.

resistance of the material. When the loading exceeds 70 phr, PVC particles are turned into carriers of stress concentration and that the toughness of the matrix is increased as the PVC content increases; therefore, the abrasion rate is decreased, and the abrasion resistance is increased [21].

3.4. Theories of rubber elasticity

According to the classical theory of rubber elasticity, new plots of the experiential data of Fig. 1 between the tensile stress, σ, versus $(\lambda^2 - \lambda^{-1})$ in the moderate range of tensile strain are presented in Fig. 8. The set of curves are found to obey the following expression:

$$\sigma = \sigma_0 + G(\lambda^2 - \lambda^{-1}) \tag{3}$$

where σ_0 is a parameter depending only on the chemical nature of the rubber matrix, and G is the rubbery modulus of the kinetic theory that depends on the degree of crosslinking [22]. The plots record a good agreement between the data from Eq. (3), which represented by solid lines, and experimental data. The interception of these lines with the stress axis at $(\lambda^2 - \lambda^{-1}) = 0$ gives the values of σ_0, while their slopes give the values of G. It is seen from the figure that, σ_0 has a constant value of 1.2 MPa for all used samples independent on the concentration of PVC. Consequently, σ_0 is a material constant, its value depends only on the chemical nature of the considered rubber and not on the crosslinking density or functionality. This term probably results from local interactions between chain segments, and by the way, may be related to the energy dissipated during deformation. The values of G are presented in Fig. 9. It is noticed that the behavior of G coincides with that of E presented in Fig. 2.

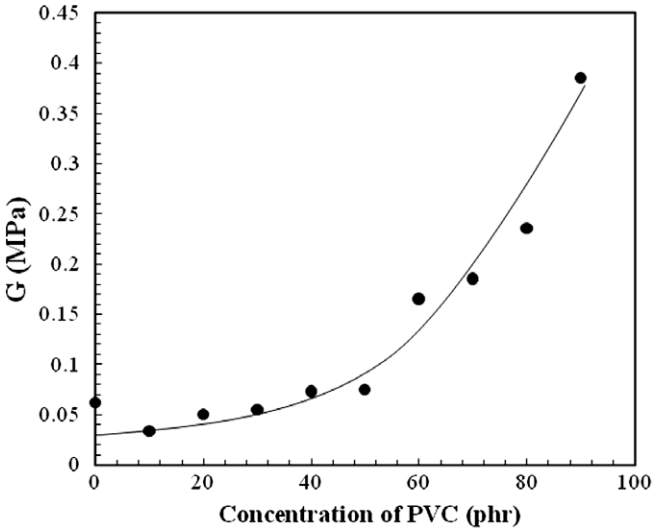

Fig. 9. Dependence of the rubbery modulus for 40FEF/(PVC–NBR) on the concentrations of PVC.

The average molecular weight M_e between crosslinks and the number of effective plastic chains per unit volume v have been calculated from the values of G according to the equation [22]

$$G = AvkT = A\frac{\rho RT}{M_e} \tag{4}$$

where ρ is the density of the rubber matrix, and R is the universal gas constant. The calculated values of M_e and v for all the studied vulcanized samples have been calculated assuming $A = 1$ [22] and are illustrated in Figs. 10 and 11 as a function of the concentration of PVC. Fig. 10 records an increase in the number of effective chains per unit volume with the concentration of PVC as that recorded by the elastic modulus E. On the other hand the behavior of M_e versus the concentration of PVC, which shown in Fig. 11, assembles that of the elongation at brake.

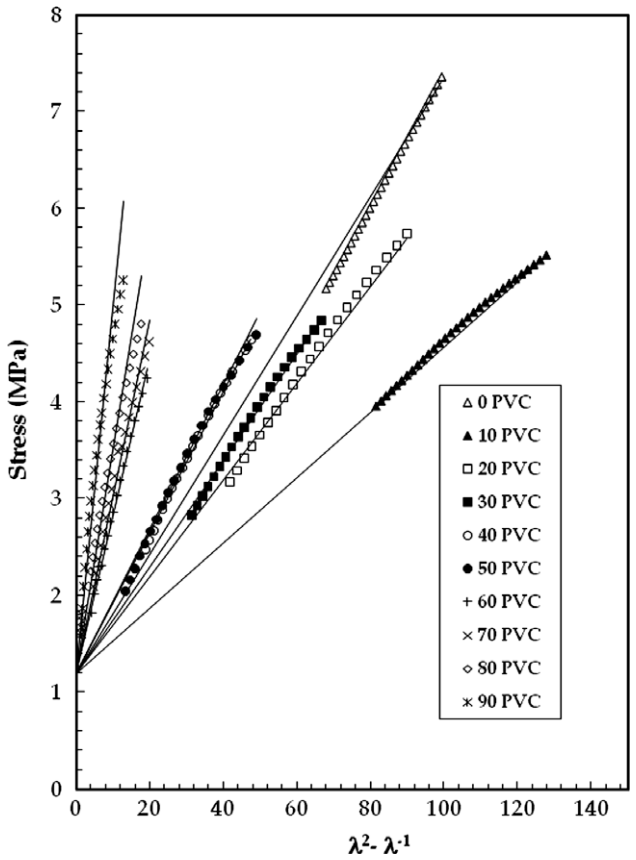

Fig. 8. Dependence of the tensile stress for 40FEF/(PVC–NBR) on $(\lambda^2 - \lambda^{-1})$ for all vulcanizates at different concentrations of PVC.

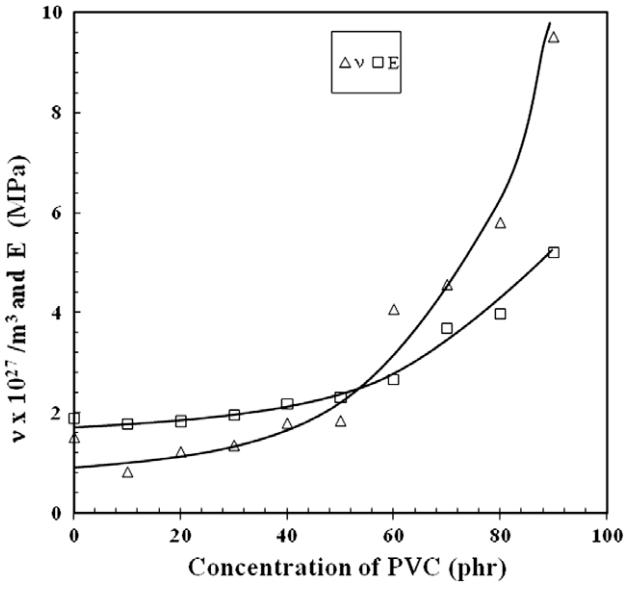

Fig. 10. Dependence of the number of effective chains per unit volume and the elastic modulus for 40FEF/(PVC–NBR) on the concentrations of PVC.

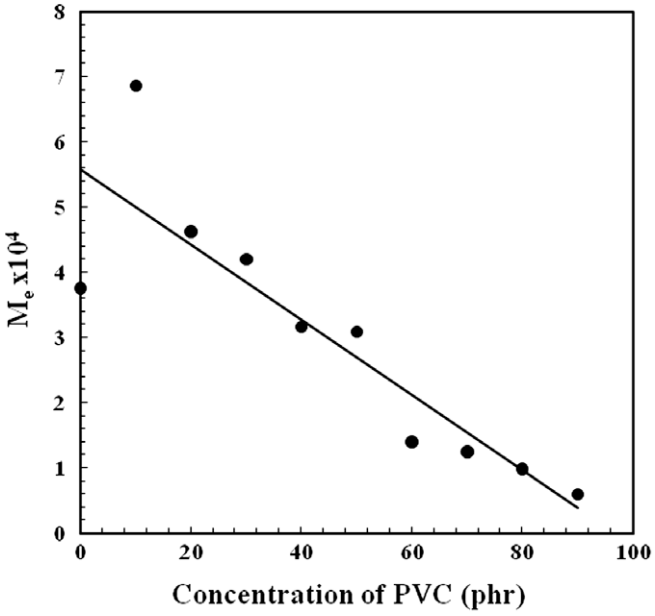

Fig. 11. Dependence of the average molecular weight for 40FEF/(PVC–NBR) on the concentrations of PVC.

3.5. Swelling

Fig. 12 shows the dependence of the degree of swelling, Q (%), on the time of swelling, t, in kerosene for 40FEF/NBR vulcanizates loaded with different concentrations of PVC. The general behavior of the curves in this figure may be approximated by an exponential function of the form:

$$Q(t) = Q_m\left[1 - \exp\left(-\frac{t}{\tau}\right)\right] \tag{5}$$

where Q_m is the maximum degree of swelling and τ is a characteristic time which depends on the concentration of PVC. Fig. 13 shows the dependence of both Q_m and τ on the concentration of PVC. It is obvious that both of them decrease as the concentration of PVC increases, which may imply that PVC particles fill the porous portions between NBR chains, which are originally small.

The increase in weight due to swelling was plotted against the square root of time (not mentioned here) and the slopes of the straight lines obtained at the early part of the curves were calculated. The penetration rate P and the average diffusion coefficient D can be calculated using the equations:

$$P = \frac{1}{2}\left(\frac{M_t}{t^{1/2}}\right)\frac{s}{M_e} \tag{6}$$

$$D = \frac{\pi}{4}P^2 \tag{7}$$

where s is the thickness of the sample and M_e and M_t are the weight uptake of the liquid at equilibrium and after time, t, respectively. The calculated values of both P and D are plotted as a function of the concentration of PVC in Fig. 14. The behavior of both of them can be divided into three regions. The first appears at loadings of PVC less than 30 phr. In this region both P and D decreases very slightly and PVC seems to be dispersed in the NBR matrix. The second region lies between 30 and 50 phr of PVC. Here, a sharp decrease is observed in both P and D owing to the continuous formation of new configurations between PVC and NBR chains in a manner, which resist the diffusion of liquid through the matrix. The last region takes place at concentration of PVC greater than 50 phr. Both P and D in this region seem to be PVC concentration

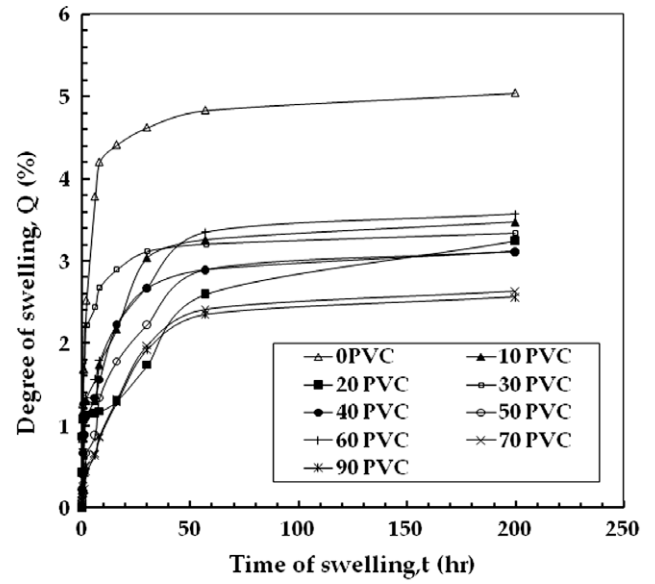

Fig. 12. Dependence of the degree of swelling on the concentration of PVC loaded 40FEF/NBR vulcanizates.

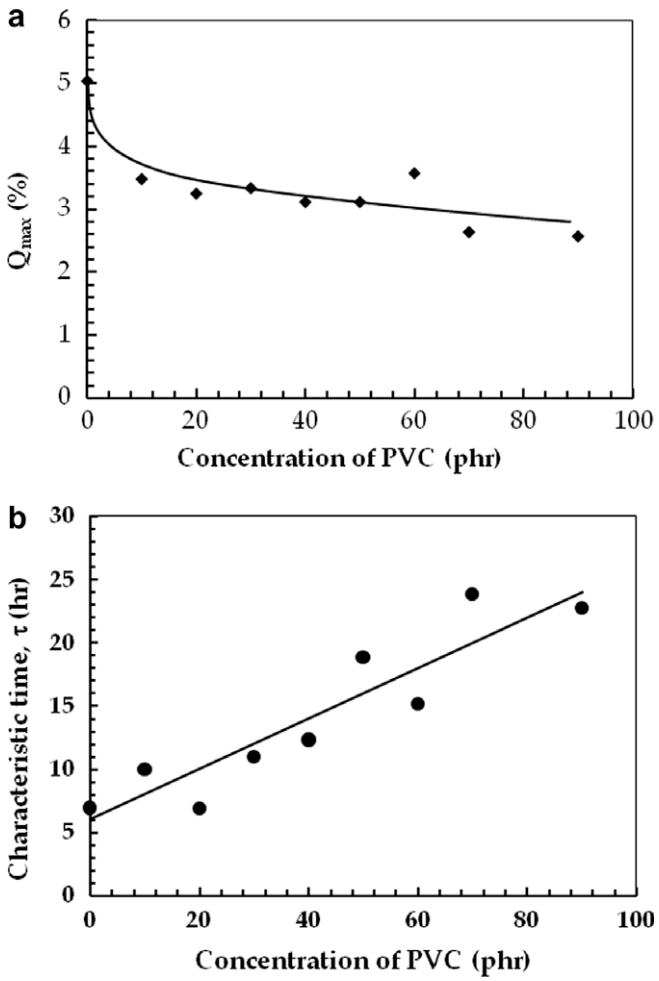

Fig. 13. Dependence of the (a) maximum degree of swelling and (b) characteristic time on the concentration of PVC loaded 40FEF/NBR vulcanizates.

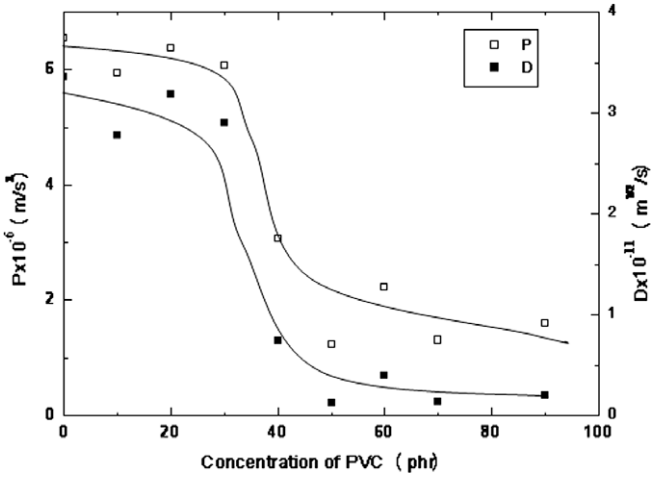

Fig. 14. Dependence of the penetration rate and the average diffusion coefficient on the concentration of PVC loaded 40FEF/NBR vulcanizates.

independent because of the formation of stable configuration of the blend.

3.6. Swelling and microhardness

The effect of immersing the studied vulcanizates which containing different concentrations of PVC on the time of immersion or the time of swelling in kerosene is shown in Fig. 15. As discussed before, the figure records the hardness degree increases when the amount of PVC increases. A very small decrease in H for all samples is recorded over the 200 h swelling in kerosene. The maximum change in the degree of hardness with time of swelling $((\frac{\Delta H}{\Delta t})_{max})$ is plotted in Fig. 16 as a function of the concentration of PVC. The figure records a linear decrease in this value at loadings of PVC ranging from zero to 50 phr. Above 50 phr, $(\frac{\Delta H}{\Delta t})_{max}$ is unchanged. This confirms the results of penetration rate and average diffusion coefficient.

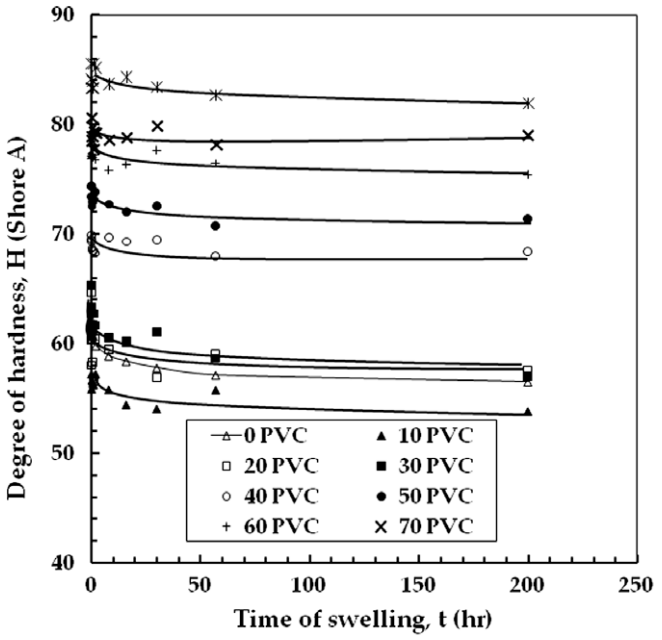

Fig. 15. Dependence of the hardness degree on the time of swelling for PVC loaded 40FEF/NBR vulcanizates.

Returning to Eq. (2) with values of m listed in Table 2 and the values of the elastic modulus illustrated in Fig. 2, the dependence of the elastic modulus on the time of swelling for all samples will be now known and illustrated in Fig. 17. Its behavior is very similar to that of the degree of hardness. The maximum change in the elastic modulus with the time of swelling $((\frac{\Delta E}{\Delta t})_{max})$ is also calculated and illustrated in Fig. 16. Its value is decreased from 0.5 MPa at zero loading of PVC to 0.2 MPa at 90 phr.

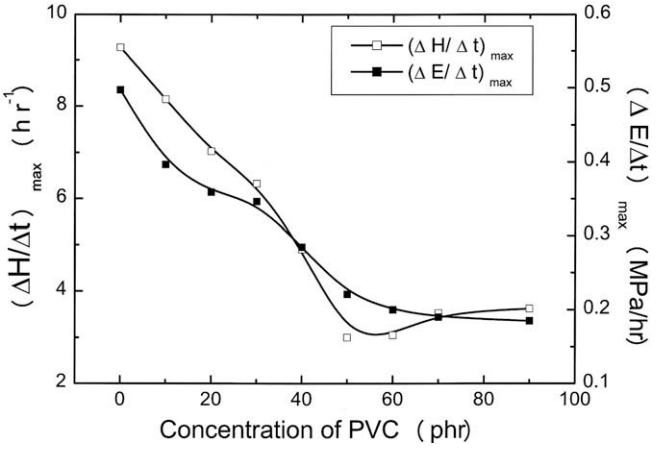

Fig. 16. Dependence of the maximum change in both hardness degree and elastic modulus with the time of swelling on the concentration of PVC loaded 40FEF/NBR vulcanizates.

Table 2
The calculated values of the conversion factor m.

PVC content (phr)	m
0	0.816
10	0.807
20	0.773
30	0.765
40	0.715
50	0.672
60	0.638
70	0.621
90	0.585

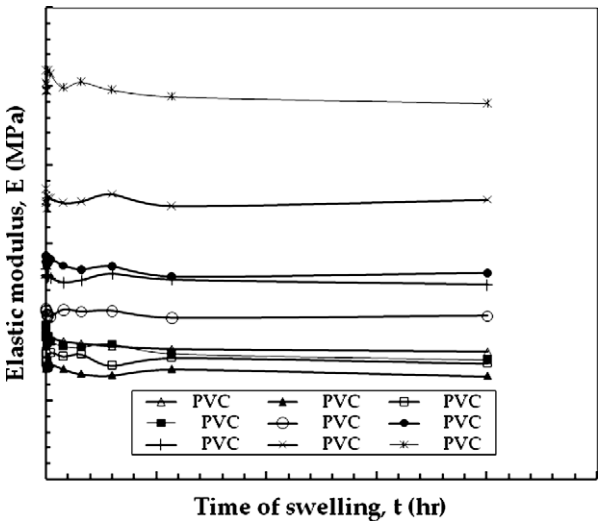

Fig. 17. Dependence of the elastic modulus on the time of swelling on the concentration of PVC loaded 40FEF/NBR vulcanizates.

4. Conclusions

One may conclude from this study that the elastic modulus, tensile strength and hardness degree increase with increasing the amount of PVC. On the other hand, the elongation at brake, abrasion resistance, maximum degree of swelling, the penetration rate and the average diffusion coefficient of kerosene decrease with increasing the amount of PVC that added to the rubber matrix. Both the rubbery modulus G and the number of effective chains per unit volume increase with increasing the concentration of PVC and agree well with the calculated values of the elastic modulus. The maximum change in both hardness degree and the elastic modulus with the time of swelling over a period of 200 h of swelling in kerosene is slightly decreased.

Acknowledgment

The authors would like to acknowledge Faculty of Science and Dean ship of scientific research, King Faisal University for providing the facilities required for the present investigation.

References

[1] Utracki LA, Walsh DJ, Weiss RA. In: Utracki LA, Weiss RA, editors. Multiphase polymers: blends and ionomers. ACS symposium series, vol. 395. Washington (DC): American Chemical Society; 1989 [chapter 1].
[2] Monakhova TV, Bogaevskaya TA, Shlyapnikov YuA. Effect of polydimethylsiloxane on oxidation of isotactic polypropylene. Polym Degrad Stabil 1999;66(1):149–51.
[3] Abu-Abdeen M, Alkhateeb A. Crosslink density and diffusion mechanisms in blend vulcanizates loaded with carbon black and paraffin wax. J Appl Polym Sci 2009;112:3232–40.
[4] Robeson LM. Applications of polymer blends: emphasis on recent advances. Polym Eng Sci 1984;24:587–97.
[5] Khanna SK, Congdon WI. Engineering and molding properties of poly(vinyl chloride), acrylonitrile–butadiene–styrene and polyester blends. Polym Eng Sci 1984;23:627–31.
[6] George KE, Joseph R, Francis J. Studies on NBR/PVC blends. J Appl Polym Sci 1986;32:2867–73.
[7] Haupt P, Lion A, Backhaus E. On the dynamic behavior of polymers under finite strains: constitutive modeling and identification of parameters. Int J Solids Struct 2000;37:3633–46.
[8] Ehlers W, Markert B. A macroscopic finite strain model for cellular polymers. Int J Plast 2003;19:961–76.
[9] Busfield JJC, Deeprasertkul C, Thomas AG. The effect of liquids on the dynamic properties of carbon black filled natural rubber as a function of pre-strain. Polymer 2000;41:9219–25.
[10] Magryta J, De Bek C, De Bek D. Mechanical properties of swelled vulcanizates of polar diene elastomers. J Appl Polym Sci 2006;99:2010–5.
[11] Medalia A. Effect of carbon black on dynamic properties of rubber vulcanizates. Rubber Chem Technol 1978;51:437.
[12] Barton JO. Effect of absorbed water on the thermal relaxation of biaxially stretched crosslinked poly(methyl methacrylate). Polymer 1979;20:1018.
[13] Ito K. A theoretical approach to the kinetics of polymer degradation in solution. J Polym Sci Polym Chem Ed 1978;16:497.
[14] Ateia E. Effect of swelling process on thermoelastic temperature change of butadiene acrylonitrile rubber filled with polyvinyl chloride. J Appl Polym Sci 2005;95:916.
[15] Hashim AS, Ong SK. Study on polypropylene/natural rubber blend with polystyrene-modified natural rubber as compatibilizer. Polym Int 2002;51:611.
[16] Sobhy MS, Mohdy MMM, Abdel-Bary EM. Effect of waste rubber powder in SBR formulations on the swelling of different organic solvents. Polym Test 1997;16:349.
[17] Mateo JL, Bosch P, Serrano J, Calvo M. Sorption and diffusion of organic solvents through photo-crosslinked SBS block copolymers. Eur Polym J 2000;36:1903.
[18] George SC, Knorgen M, Thomas S. Effect of nature and extent of crosslinking on swelling and mechanical behavior of styrene–butadiene rubber membranes. J Membr Sci 1999;163:1.
[19] Abu-Abdeen M, Abdalaziz AA, Sedky A. Mechanical behavior and microhardness of swollen natural rubber loaded with carbon black. J Appl Polym Sci 2008;109:3361.
[20] Gunasunderi R, Chantara TR, Nor AI, Mohammad ZAbR, Wan MZWY. Enhancement of PVC/ENR blend properties by poly(methyl acrylate) grafted oil palm empty fruit bunch fiber. J Appl Polym Sci 2008;110:368–75.
[21] Tan J, Ding YM, He XT, Liu Y, An Y, Yang WM. Abrasion resistance of thermoplastic polyurethane materials blended with ethylene–propylene–diene monomer rubber. J Appl Polym Sci 2008;110:1851–7.
[22] Abu-Abdeen M. Degradation of the mechanical properties of composite vulcanizates loaded with paraffin wax. J App Polym Sci 2001;81:2265–70.